

# Ionic Liquid Potential to Recycle Polymeric Waste: An Experimental Investigation

Waleed Ahmed<sup>a\*</sup> , Rabah Khenata<sup>b</sup>, Sidra Siraj<sup>c</sup>, Y. Al-Dourid<sup>d,e</sup>

<sup>a</sup>United Arab Emirates University, College of Engineering, Engineering Requirements Unit, Al Ain, United Arab Emirates

<sup>b</sup>Mascara University, Faculty of Sciences & Technology, Algeria

<sup>c</sup>United Arab Emirates University, College of Engineering, Chemical Engineering Department, Al Ain, United Arab Emirates

<sup>d</sup>University of Malaya, Nanotechnology and Catalysis Research Center (NANOCAT), 50603 Kuala Lumpur, Malaysia

<sup>e</sup>Bahcesehir University, Faculty of Engineering and Natural Sciences, Department of Mechatronics Engineering, 34349 Besiktas, Istanbul, Turkey

Received: June 20, 2020; Revised: September 18, 2020; Accepted: October 23, 2020.

The impact of ionic liquid (IL) solution on the recycling process of polyethylene terephthalate (PET) waste containers used to store drinking water, with a focus on optimizing the added percentage and processing conditions of IL was studied. Characterization using differential scanning calorimeter (DSC), thermogravimetric analyzer (TGA), Fourier transform infrared spectroscopy (FTIR) and nano-indentation tests were performed. Generally, an increase in the degradation temperatures was observed with increasing IL%. Since they were quite comparable, their good thermal stability could be considered. An increase in the hardness was noticed from 0.41 at 0% to 0.45 at a 2% IL solution. A rise in the modulus of elasticity was also observed from 5.5 GPa at 0% to 8 GPa at 2% IL solution. Although there has been some improvement in the properties of the IL blends, limitations such as IL cost and their effective recycling remains a challenge and needs more efforts to fully explore their potential.

**Keywords:** Recycling, PET, mechanical properties, ionic liquid.

## 1. Introduction

Plastic or polymeric consumption has increased rapidly due to the change in the customer lifestyle that has led to the progressive escalating of waste production. Researchers are stimulated to work on finding environmental solutions to resolve the problem of the accumulating and the increasing waste of polymeric materials to preserve the natural resources of the earth. The amount of volatile organic compounds (VOCs) industrially used is on the rise as VOCs are mainly utilized as solvents in solution polymerization due to their compatibility with monomers and ease of separation. However, over the years, there have been health and environmental risks associated with VOCs worldwide, hence alternative solutions that could replace the VOCs are being explored.

Ionic liquids (ILs), or molten salts, are a combination of cations and anions that melt below 100°C. They are environmentally benign and have shown good potential as replacements to VOC's in several applications. Due to their unique properties such as high chemical stability, low vapor pressure, low flammability, high conductivity, and excellent solubility towards organic compounds, ILs are being explored extensively in the field of polymerization<sup>1,2</sup>. Since a significant advantage of ILs is their recyclability, therefore, ILs containing dissolved catalysts are frequently used in reaction cycles<sup>3</sup>.

One of the most consumed plastics is polyethylene terephthalate, which is popularly known as PET, the food-

grade polymer. PET has many advantages that make it one of the most demanding plastics, for instance, its high melting temperature, resistance to organic chemicals, resistance to moisture, and its ability to improve mechanical properties. As the consumption of PET is expected to grow up to over 500 billion production units by 2021<sup>4</sup>, the need to study more efficient and eco-friendly methods to dispose of the waste produced by the rising PET consumption must be explored.

There are various methods physical or chemical, to handle the recycling of polymeric waste, especially for PET. However, only chemical recycling promotes sustainability as it results in the production of raw materials that are originally produced from PET. Many chemical processes have been adopted to recycle PET depolymerization, such as alcoholysis, hydrolysis, and glycolysis, with glycolysis being one of the most adopted processes used for R-PET.

Glycolysis can be termed as a molecular depolymerization process by transesterification between PET ester groups and a diol, usually, ethylene glycol (EG) in excess, to obtain bis (2-hydroxyethyl) terephthalate (BHET) as the monomer<sup>5</sup>. Glycolysis is found to be an efficient process for post-consumer PET (PET-pc) chemical recycling, as it can be conducted efficiently at comparatively less harsh operating parameters and low pressures to other processes. However, this reaction is reported to be slower in the absence of catalyst<sup>6,7</sup>, hence the use of catalysts for this process is highly promoted. Many catalysts like titanium-phosphate, metal acetates,

\*e-mail: w.ahmed@uaeu.ac.ae

carbonate, metal oxide, solid superacids, and sulfates have been studied for the glycolysis of PET<sup>8,9</sup>. Additionally, studies also reveal that ILs have been widely used as catalysts for the glycolysis of PET, with 100% conversion of PET and 59.2% selectivity of BHET being achieved in the existence of Fe-containing magnetic ionic liquid, making ILs as well outstanding candidates to be used for the glycolysis of PET<sup>10-12</sup>. Another key advantage of ionic liquids over the conventionally-used catalysts such as metal acetates is that the purification of the products obtained from glycolysis is relatively simpler<sup>13</sup>. The structure of the chosen ionic liquid; 1-Butyl-3-methylimidazolium Hydroxide [bmIm]OH is illustrated in Figure 1. The main reason behind choosing this particular IL as it's very stable and task-specific, promoting Michael addition without requiring any additional solvents and resulting in a high product yield<sup>14</sup>. An example of the possible mechanism of the glycolysis reaction of PET in the presence of metal-containing ionic liquids is represented in Figure 2<sup>14</sup>.

The ease of recycling this widely used commodity polymer through ILs has led researchers to study the effect of mixing of recycled PET (R-PET) with other materials to investigate the mechanical and chemical impact on the new mixture. The influence of (R-PET) powder on thermal properties, fatigue life, and surface morphology of halloysite nanotubes (HNTs) and silica filled natural rubber composites have widely been studied<sup>15,16</sup>. Results indicate a decrease in the fatigue life of the natural rubber composites with the substitution of these two fillers by R-PET. In another study,

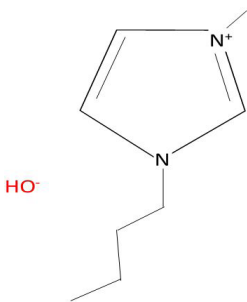


**Figure 1.** Chosen ionic liquid structure.

R-PET enhanced thermal resistance, tensile strengths, and ductility when mixed with concrete material. PET fibers are also reported to increase fracture toughness, impact strength, split tensile strength, flexural strength, and compressive strength when produced in blends with other polymeric materials as well<sup>17,18</sup>. Evidently, the addition of PET has affected the material properties, mainly improving the mechanical integrity and thermal resistivity, thereby making PET a high-quality polyester to recycle consecutively. Additionally, repeated recycling of PET is reported to have produced comparable results to virgin PET in terms of material characteristics, supporting its recycling as a good alternative for plastic waste disposal<sup>19</sup>.

Since PET is extensively reported to impact the mechanical properties<sup>20</sup>, in this study, PET recycled bottles were collected to study the impact of ionic liquids on the mechanical properties of the blends. The characteristics of the prepared PET-IL blends were analyzed to determine the optimum mixing ratio that enhances mainly the thermal and mechanical properties of the mixture.

## 2. Materials and Methods

### 2.1 Sample Preparation

The ionic liquid used in this analysis was prepared carefully based on literature<sup>14</sup>. The procedure to prepare this ionic liquid is as follows. Solid potassium hydroxide (40 mmol, 2.3 g) was added into a solution of [bmIm]Br (40 mmol, 8.8 g) in 20 mL of dry methylene chloride solution. This mixture was then vigorously stirred at room temperature for 10 hours. The precipitated potassium bromide (KBr) was then filtered off, and the filtrate was evaporated to leave the crude to reside [bmIm]OH as a viscous liquid which was washed with ether (2-20 mL) and then dried at 90°C for another 10 hours to prepare the ionic liquid. Next, to add PET shreds, unified type of PET water bottles was collected from the same source, and the collected bottles were cleaned using water and then dried employing a drying oven to remove any residual moisture<sup>21</sup>, preventing potential hydrolysis of PET in the melt phase that could reduce its molecular weight<sup>22</sup>. PET must be dry just before processing, and amorphous PET requires crystallizing before drying so that the particles don't stick together as they go through the glass transition.

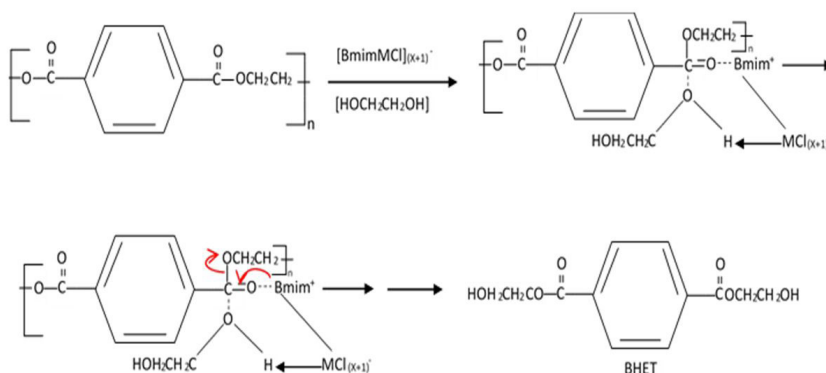


**Figure 2.** Possible mechanism scheme of the glycolysis reaction of PET in the presence of metal-containing ionic liquids.

The dried samples were cut into smaller pieces and placed in a shredding machine to shred to the output size of 5 mm x 5 mm. The shreds were then mixed with the prepared ionic liquid at ~20°C for 20-30 minutes until homogeneity was achieved. A set of five varying mixing ratios was adopted in this analysis (i.e., ratio 2% IL, 3% IL, 5% IL, 7% IL, and 10% IL). Weighed amounts of the sample blends were melt blended in a twin-screw extruder (MiniLab HAAKE Rheomex CTW5, Germany) for 5 minutes at 40°C and a screw speed of 50 rpm. The extruded material was prepared under room temperature. Each sample was made from one batch and collected for further analysis and investigation. A simple

schematic of the process is shown below in Figure 3 and the extruder setup is shown in Figure 4.

## 2.2 Differential scanning calorimetry (DSC)

Thermal properties of PET blends were determined using a modulated differential scanning calorimeter (MDSC) (Discovery DSC 25, TA Instruments, USA). About 5-10 mg sample was heated from 25°C to 200°C at a heating rate of 40°C/min to remove the thermal history of the polymer. The glass transition temperature ( $T_g$ ) was recorded from 85°C-110°C, as well as the melting temperatures ( $T_m$ ) were recorded from the second heat from 25°C - 400°C at

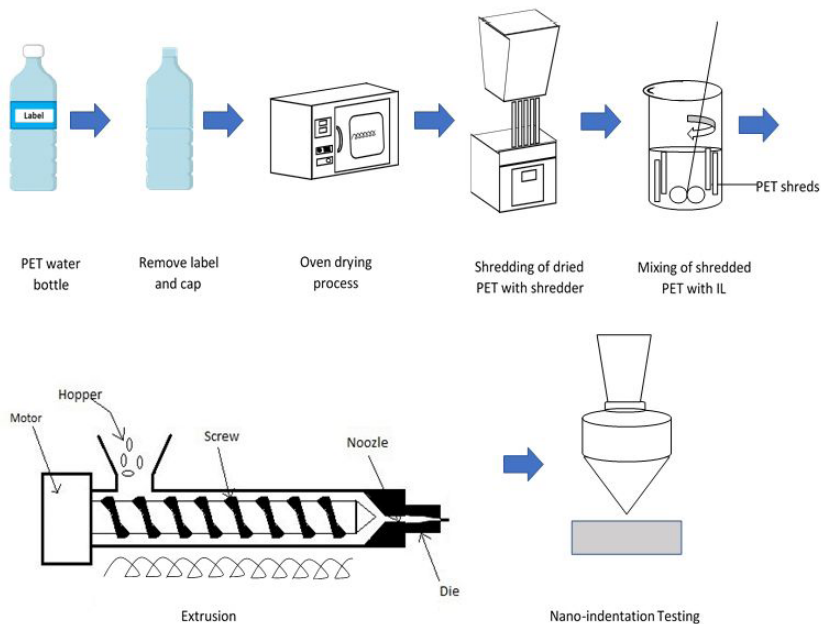


Figure 3. Process Schematic.



Figure 4. Extruder setup.

10°C/min. All experiments were carried out under an inert nitrogen atmosphere.

### 2.3 Thermal Gravimetric Analysis (TGA)

Thermogravimetric analysis (TGA) was carried out in a thermogravimetric analyzer (Q-50, TA Instruments, USA). Approximately, 10-15 mg sample was heated from 20°C to 800°C at a heating rate of 20°C/min under nitrogen atmosphere (100 mL/min).

### 2.4 Nano-indentation

Nanoindentation was used to estimate the mechanical properties (hardness and the modulus of elasticity (Y)) of the neat PET, pure ILs, and the prepared samples as well. The nanoindentation tests were performed using a three-sided pyramid diamond tip (Berkovich type) nanoindenter<sup>22</sup>. A constant displacement of (i.e., 0.0167 mN/s) was applied to perform the nanoindentation experiments. A fixed applied load was retained for 30 seconds with a maximum value of 1 mN. Each time the indenter approached a specific depth of (i.e., 1827nm) into the surface, the load was removed to avoid any creep that could influence the unloading performance. Moreover, the indenter was removed from the surface at the same former displacement rate whenever a maximum of 10% load was achieved. In addition to that, a constant displacement rate was also considered in the tests to minimize the influence of the hardening on the acquired measurements<sup>23</sup>. A set of five indents were applied to each sample, with over 50 μm of the distance between each indent. The hardness and the modulus of elasticity (Y) were calculated through the load-displacement figure through the equation presented in the literature<sup>24</sup>.

The hardness can be estimated using Equation 1<sup>25</sup>

$$H = \frac{P_{\max}}{A} = \frac{P_{\max}}{24.5h_c^2} \quad (1)$$

Where,  $P_{\max}$ : the measured value of the applied load in an indentation cycle (maximum depth of the penetration (h)), A: the contact area (i.e., projected),  $h_c$ : the indentation depth (i.e., contact) that is estimated by:

$$h_c = \frac{h - 0.75P_{\max}}{S} \quad (2)$$

Where S: (dp/dh) is the slope of the initial section of the unloading curve at  $h = h_{\max}$ , and a constant value of 0.75 is considered that is dependent on the indenter geometry.

Using the initial unloading contact stiffness, the Young's modulus of the sample was estimated. The correlation between contact area, contact stiffness, and Young's modulus could be determined using the following relationship presented in Equation 3<sup>25</sup>:

$$S = 2\beta E_r \left( \frac{A}{\pi} \right)^{1/2} \quad (3)$$

Where,

$\beta$ : a geometry constant. The parameter  $\beta$  being governed by the indenter itself,  $\beta = 1.034$  for a Berkovich indenter, whereas

$E_r$  is the reduced elastic modulus, by considering the elastic deformation of the indenter as well as the tested sample.

To calculate the contact stiffness, elastic modulus, and the contact area. The parameters can be calculated accurately from the load against the displacement diagram that was drawn over the measurement of the indentation process. The sample's elastic modulus ( $E_s$ ) was then estimated using Equation 4<sup>22</sup>:

$$E_s = (1 - \nu_s^2) \left\{ \frac{1}{E_r} - \frac{(1 - \nu_i^2)}{E_i} \right\}^{-1} \quad (4)$$

where  $\nu_s$ : Poisson's ratios of the sample which is estimated for semi-crystalline polymeric materials ( $\nu_s=0.35$ )<sup>26</sup>,  $\nu_i$ : Poisson's ratio of the diamond indenter ( $\nu_i=0.07$ )<sup>27</sup>,  $E_i$ : Elastic modulus of the diamond indenter = 1141 GPa which was considered in all calculations.

### 2.5 FTIR analysis

The FTIR was performed on all the samples prepared using a transmission infrared spectrophotometer (NEXUS-470, Thermo Nicolet Corporation), at room temperature. After scanning the background, the sample was directly placed in the sample holder after scanning the background. The results of the absorption spectra were recorded in the range of 4000  $\text{cm}^{-1}$ -400 $\text{cm}^{-1}$  in a period of 32 scans, with a resolution of 2  $\text{cm}^{-1}$ . The characteristic absorptions bands of the prepared blends were registered.

## 3. Results and Discussions

### 3.1 DSC analysis

Figure 5 demonstrates the DSC results obtained for the PET-ionic liquid mixtures after extrusion to mainly evaluate the peak melting temperatures ( $T_m$ ) of the prepared blends. The melting peak of the PET is observed at around 227°C for PET. The melting peaks of PET blends decreased slightly to 226.2°C for 10%IL. As the %IL is increased, a shifting trend in the DSC curve is observed. This shift is associated with a decrease in the melting temperatures. This behavior could be possibly explained due to the reduction of the PET molecules with increasing IL% into the matrix. Additionally, this also corresponds to the fact that PET crystallinity is reduced thereby enhancing the mobility of the PET segments<sup>28</sup>. The low melting temperature of PET compared to other polymers corresponds to its low crystallization rate which is one of the key barriers concerning its use as an engineering thermoplastic, hence an additive could be a good idea to incorporate to increase the nucleation sites which in turn could increase the crystallization rate<sup>29</sup>. Moreover, the glass transition temperature ( $T_g$ ) value of polymers is highly affected by the crystallinity<sup>30</sup>, which is in turn is related to the  $T_m$  value of the polymers. As no significant variation in  $T_m$  is observed for the blends, hence it can be stated that the  $T_g$  values for the blends did not vary significantly as well, and fluctuated in the ranges of 85°C-110°C (see Figure 5). Table 1 reports all the melting temperatures for the prepared PET-IL blends.



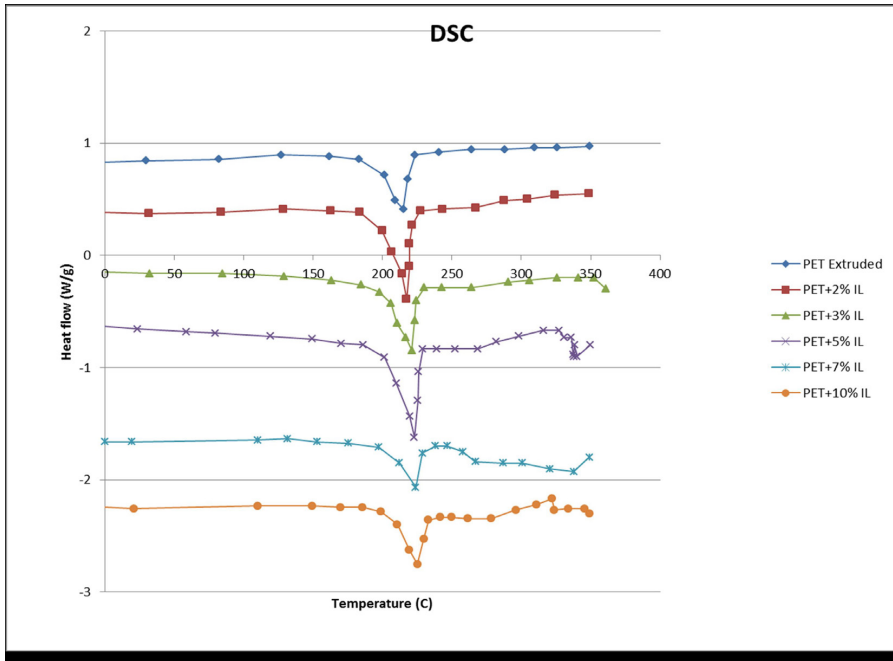


Figure 5. DSC data for prepared PET-IL blends.

Table 1. Melting temperatures of prepared PET-IL blends.

PERCENTAGE IL (%)	$T_d$ (°C)	Weight loss at 100°C (%)	Weight loss at 500°C (%)
0	215.01	14.44	85.56
2	217.30	13.38	86.64
3	221.11	12.24	87.77
5	222.80	10.74	89.27
7	223.90	9.08	90.93
10	225.10	8.09	91.91

Table 2. TGA data for prepared PET-IL blend

Percentage IL (%)	0	2	3	5	7	10
$T_m$ (°C)	226.9	228.5	228.1	227.0	226.5	226.2

### 3.2 TGA analysis

The thermal stability of the PET-IL blends was also analyzed using TGA. The TGA tests were done on neat PET as well as on all the prepared five samples of the PET-IL blends. As illustrated in Figure 6, the neat PET showed the highest thermal stability with the corresponding degradation temperature ( $T_d$ ) at 215°C, with the majority of the degradation starting beyond 400°C. Moreover, the PET-IL blend at 5%IL appears to be degrading the fastest, and this could be related to the reaction being completed the fastest at that weight percent. A similar trend is mentioned in the literature as well<sup>10</sup>. The weight loss at 100°C can be implied mainly caused due to moisture, varying from 14% for pure PET to 8% for PET blends prepared at 10% IL. Additionally, the increasing degradation temperatures can be attributed to the volatility of the added IL at elevated temperatures, which is

also reported in literature<sup>28</sup>. However since the degradation temperatures are fairly similar for all the prepared blends, their thermal stability can be considered. Table 2 reports the TGA data for all the prepared blends. Combining DSC and TGA data reveals that the product decomposes before it melts, concluding that the product of degradation deteriorates relatively easier than PET.

### 3.3 Nanoindentation test

The hardness and elastic modulus were calculated using the loading and the unloading curves of tested samples which are illustrated in Figure 7 respectively,

The mechanical properties of polymers are shaped by the significant role of the plasticizer added in the blend. It is well reported that the tensile strength decreases with increasing plasticizer composition. A similar trend is also reported for the elongation at the breakpoint<sup>30</sup>. As shown in Figure 8, there is a sharp increase in the Young's modulus from 5.5 GPa at 0% to 8 GPa at 2%IL. This increase in the elastic modulus could be due to the molecules of IL initially trapping and filling in the gaps in the matrix, which increases the mechanical characteristics. However, beyond this point, a steady decrease in Young's modulus was observed from 8 GPa at 2% IL to 4.5 GPa at 10% IL respectively.

The same decreasing trend (shown in Figure 9) was also observed in the hardness values obtained for the prepared samples, from 0.45 GPa at 2% IL to lower than 0.3 GPa at 10% IL respectively. The decreasing trend can be explained by the reduction of the intramolecular forces in PET with increasing IL%. Additionally, the low-molecular-weight small molecules of the IL may get entrapped in between the matrix or chains of the PET, thereby increasing the free volume and spacing, which allows polymeric chains to glide past each other even at lower temperatures leading to

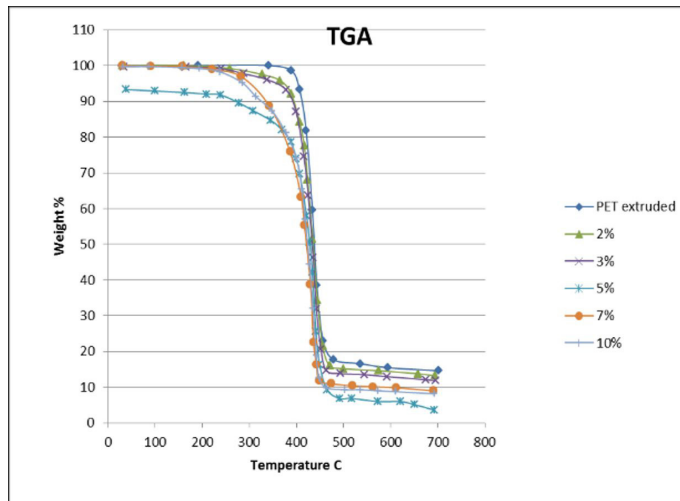


Figure 6. TGA data for prepared PET-IL blends.

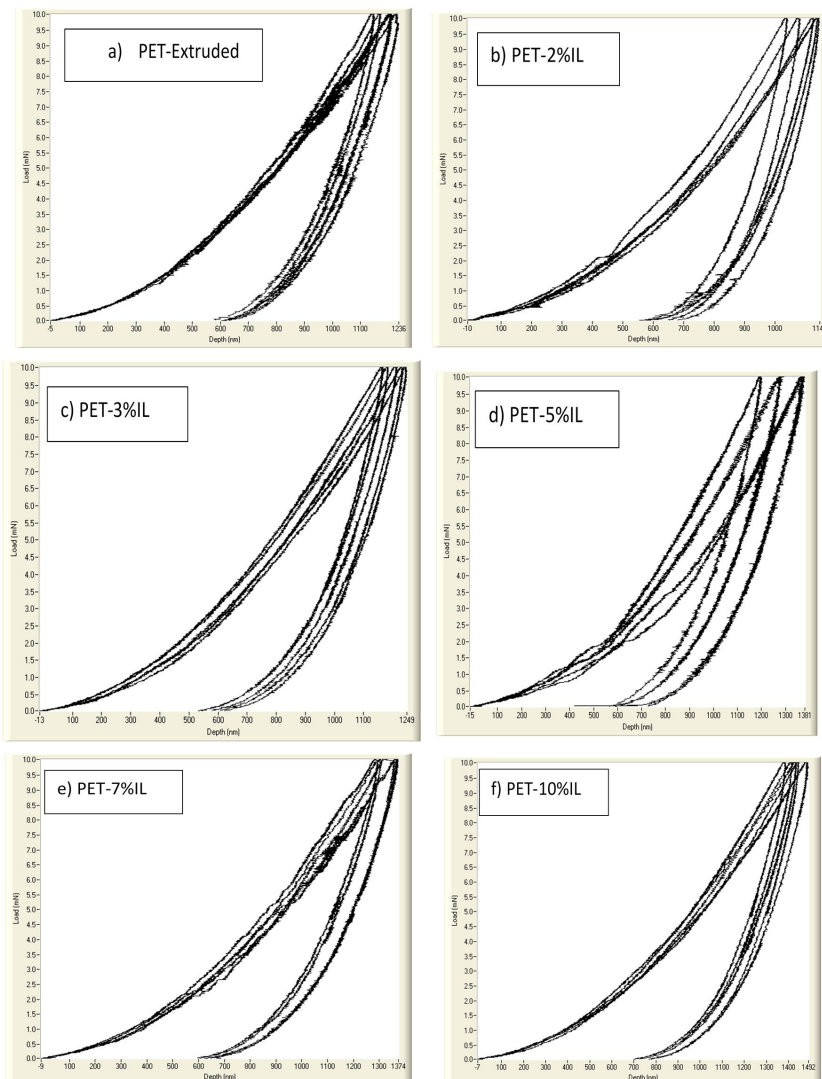


Figure 7. Loading-unloading curves of the nanoindentation tests for the PET-IL blends (a) PET (b) PET-2% IL (c) PET-3%IL (d) PET-5%IL (e) PET-7% IL (f) PET-10%IL.

breakage<sup>28</sup>. This is also observed for many polymer blends and is explained as beyond a certain percentage value, the random agglomeration of particles weakens the polymer matrix to a point, causing uneven crystallization and leading to their brittle nature which leads to a decrease in the tensile strength and consequently to their hardness value as well<sup>15</sup>. The Young's modulus and the hardness of the PET-IL blends are illustrated in Figures 8 and 9 respectively.

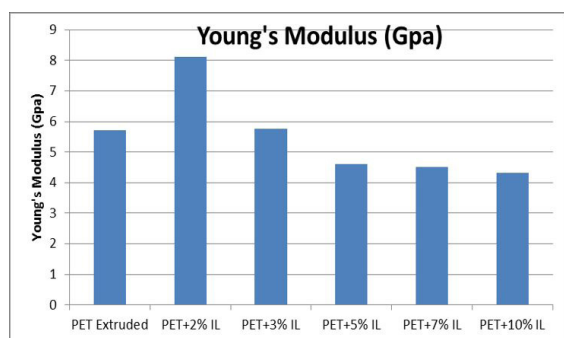


Figure 8. The Young's modulus of the prepared PET-IL blends.

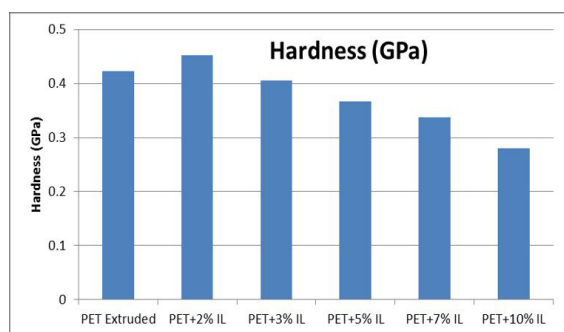


Figure 9. The hardness of the prepared PET-IL blends.

### 3.4 FTIR analysis

In order to indicate the existence of specific chemical species in the tested specimens, Fourier transforms infrared spectroscopy was conducted. The presence of peaks in the  $1000\text{ cm}^{-1}$  and  $2000\text{ cm}^{-1}$  was witnessed for all samples corresponding to the presence of PET for all samples as reported in the literature as well<sup>31,32</sup>, which are mainly associated with the stretching of the carbon-oxygen ester bonds<sup>33</sup>. Moreover, similar absorption trends were witnessed for all the prepared blends. A distinct peak between  $3000\text{ cm}^{-1}$  and  $4000\text{ cm}^{-1}$  was obtained in the case of neat PET as well as in all the prepared blends, signifying no major structural change in the basic polymeric structure of PET itself. These peaks can be associated with the OH intermolecular hydrogen bonding<sup>34</sup>. It is shown stretching band, asymmetric and symmetric around  $1800$  and  $1200\text{ cm}^{-1}$ . Very weak bending vibrations appeared at  $2950$ , and  $1450\text{ cm}^{-1}$ . Medium-strong band position in the range of  $1100\text{ cm}^{-1}$  due to stretching vibrations of PET. For 2%, a weak absorption band presents at  $1750\text{ cm}^{-1}$ . Very weak bending vibration appeared at  $1150\text{ cm}^{-1}$ . Medium-strong band positions in the range,  $2950$  and  $1500\text{ cm}^{-1}$  due to stretching vibrations of the sulfate group. While for 3%, a weak absorption band presents at  $1780\text{ cm}^{-1}$ . Very weak bending vibration appeared at  $1180\text{ cm}^{-1}$ . Medium-strong band positions in the range,  $2980$  and  $1480\text{ cm}^{-1}$  due to stretching vibrations. For 5%, a weak absorption band present at  $1800\text{ cm}^{-1}$ . Very weak bending vibration appeared at  $1200\text{ cm}^{-1}$ . Medium-strong band positions in the range,  $3000$  and  $1500\text{ cm}^{-1}$  due to stretching vibrations. For 7%, a weak absorption band present at  $1800\text{ cm}^{-1}$ . Very weak bending vibration appeared at  $1200\text{ cm}^{-1}$ . Medium-strong band positions in the range,  $3010$  and  $1510\text{ cm}^{-1}$  due to stretching vibrations. And for 10%, a weak absorption band present at  $1820\text{ cm}^{-1}$ . Very weak bending vibration appeared at  $1220\text{ cm}^{-1}$ . Medium-strong band positions in the range,  $3020$  and  $1520\text{ cm}^{-1}$  due to stretching vibrations. FTIR of neat PET and all the samples are shown in Figure 10.

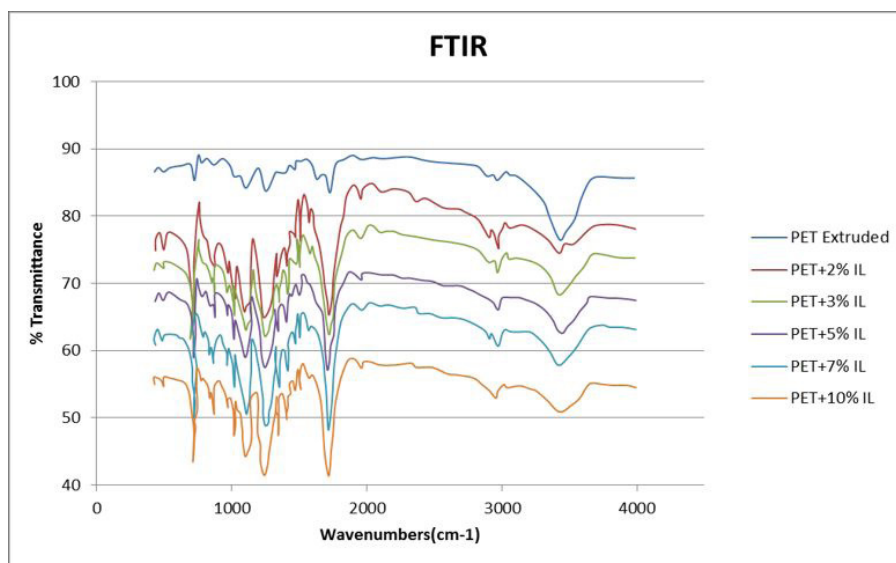


Figure 10. FTIR spectroscopy for neat PET and all prepared PET-IL blends.

## 4. Conclusion

Due to the massive increase in plastics wastes especially the PET, many approaches have been investigated aiming to contribute to minimizing the environmental impact of the plastics waste and to find innovative and environmentally friendly solutions especially since plastics in general, are easily separable from other solid wastes<sup>35</sup>. This investigation reveals a positive impact of the ionic liquid mixed with waste PET on the thermal properties of the prepared blends. Almost similar melting temperatures, varying between 226°C-229°C were obtained for all the prepared blends, which corresponds to good thermal stability, and an increase in their degradation temperatures from 215°C to 225°C was obtained for all the blends prepared. From this thermal analysis, it could be concluded that the product of degradation of the reaction is easily decomposed compared to PET. A similar trend is reported in the literature as well<sup>11</sup>. In terms of their mechanical properties, an increase in Young's modulus from 5.5 GPa to 8 GPa, and hardness from 0.41 to 0.45 was observed as the percentage of the ionic liquid mixture was increased up to 2% IL compared to the neat PET respectively, suggesting improved mechanical performance up to this point. This can be concluded being a result of their corresponding additive mechanical properties. However, beyond 2% IL, the samples exhibited a decrease in their mechanical properties suggesting a potential weakening of the structure with increasing IL percentage as IL could start to fill the free volume in between the matrix and suppressing PET segmental mobility<sup>36</sup>. FTIR suggests no changes being made to the polymeric structure, indicating the absence of any chemical reactions occurring between the chosen IL and PET and implying that this process is only based on the breaking of the chemical bonds, promoting their chemical stability as reported in the literature as well<sup>11</sup>. Considering the importance of good waste PET disposal, this work contributes to a better understanding of the usage of ionic liquids in preparing blends from recycled PET bottles that could be potentially reused with comparable mechanical properties. However, extensive research can further be conducted on varying the IL percentages between 0% IL-2%IL, to gain a fundamental understanding of the mechanical and thermal properties between this specific range.

## 5. References

- Mallakpour S, Dinari M. High performance polymers in ionic liquid: a review on prospects for green polymer chemistry. Part II: polyimides and polyesters. *Iranian Polym J*. 2011;20(4):259-79.
- Gorke J, Srien F, Kazlauskas R. Toward advanced ionic liquids. Polar, enzyme-friendly solvents for biocatalysis. *Biotechnol Bioprocess Eng; BBE*. 2010;15(1):40-53.
- Kubisa P. Ionic liquids as solvents for polymerization processes: progress and challenges. *Prog Polym Sci*. 2009;34(12):1333-47.
- Statista. PET global bottle production 2021 [Internet]. New York: Statista; 2020 [cited 2020 June 14]. Available from: <https://www.statista.com/>
- López-Fonseca R, Duque-Ingunza I, de Rivas B, Arnaiz S, Gutiérrez-Ortiz JI. Chemical recycling of post-consumer PET wastes by glycolysis in the presence of metal salts. *Polym Degrad Stabil*. 2010;95(6):1022-8.
- Troev K, Grancharov G, Tsevi R, Gitsov I. A novel catalyst for the glycolysis of poly(ethylene terephthalate). *J Appl Polym Sci*. 2003;90(4):1148-52.
- Pingale ND, Palekar VS, Shukla SR. Glycolysis of postconsumer polyethylene terephthalate waste. *J Appl Polym Sci*. 2010;115(1):249-54.
- Shukla SR, Harad AM. Glycolysis of polyethylene terephthalate waste fibers. *J Appl Polym Sci*. 2005;97(2):513-7.
- Shukla SR, Kulkarni KS. Depolymerization of poly(ethylene terephthalate) waste. *J Appl Polym Sci*. 2002;85(8):1765-70.
- Wang H, Liu Y, Li Z, Zhang X, Zhang S, Zhang Y. Glycolysis of poly(ethylene terephthalate) catalyzed by ionic liquids. *Eur Polym J*. 2009;45(5):1535-44.
- Wang H, Li Z, Liu Y, Zhang X, Zhang S. Degradation of poly(ethylene terephthalate) using ionic liquids. *Green Chem*. 2009;11(10):1568-75.
- Wang H, Yan R, Li Z, Zhang X, Zhang S. Fe-containing magnetic ionic liquid as an effective catalyst for the glycolysis of poly(ethylene terephthalate). *Catal Commun*. 2010;11(8):763-7.
- Khoonkari M, Haghghi AH, Sefidbakht Y, Shekoochi K, Ghaderian A. Chemical recycling of PET wastes with different catalysts. *Int J Polym Sci*. 2015, 2015:124524.
- Ranu BC, Banerjee S. Ionic liquid as catalyst and reaction medium. the dramatic influence of a task-specific ionic liquid, [bmIm]OH, in Michael addition of active methylene compounds to conjugated ketones, carboxylic esters, and nitriles. *Org Lett*. 2005;7(14):3049-52.
- Yue QF, Yang HG, Zhang ML, Bai XF. Metal-containing ionic liquids: highly effective catalysts for degradation of poly(ethylene terephthalate). *Adv Mater Sci Eng*. 2014;2014:454756.
- Hayeemasae N, Ismail H, Azura AR. The influence of recycled poly(ethylene Terephthalate) powder on fatigue life, thermal stability, and morphology of Halloysite Nanotubes (HNTs) and precipitated silica filled natural rubber composites. *KEM*. 2011;471-472:628-633.
- Nabil H, Ismail H, Rashid AA. Effects of partial replacement of commercial fillers by recycled poly(ethylene terephthalate) powder on the properties of natural rubber composites. *J Vinyl Addit Technol*. 2012;18(2):139-46.
- Pelisser F, Montedo ORK, Gleize PJP, Roman HR. Mechanical properties of recycled PET fibers in concrete. *Mater Res*. 2012;15(4):679-86.
- Pires HM, Mendes LC, Cestari SP, Pita VJRR. Effect of weathering and accelerated photoaging on PET/PC (80/20 wt/wt%) melt extruded blend. *Mater Res*. 2015;18(4):763-8.
- Mancini SD, Zanin M. Recyclability of PET from virgin resin. *Mater Res*. 1999;2(1):33-8.
- Awaja F, Pavel D. Recycling of PET. *Eur Polym J*. 2005;41(7):1453-77.
- Oliver WC, Pharr GM. An improved technique for determining hardness and elastic modulus using load and displacement sensing indentation experiments. *J Mater Res*. 1992;7(6):1564-83.
- Beake BD, Chen S, Hull JB, Gao F. Nanoindentation Behavior of Clay/Poly(Ethylene Oxide) Nanocomposites. *J Nanosci Nanotechnol*. 2002;2(1):73-9.
- Fang T-H, Chang W-J. Nanomechanical properties of copper thin films on different substrates using the nanoindentation technique. *Microelectron Eng*. 2003;65(1):231-8.
- Sneddon IN. The relation between load and penetration in the axisymmetric boussinesq problem for a punch of arbitrary profile. *Int J Eng Sci*. 1965;3(1):47-57.
- Simmons G. Single crystal elastic constants and calculated aggregate properties. Texas: Southern Methodist Univ Dallas Tex; 1965.
- Cuq B, Aymard C, Cuq J-L, Guilbert S. Edible packaging films based on fish myofibrillar proteins: formulation and functional properties. *J Food Sci*. 1995;60(6):1369-74.



28. Mohsin MA, Abdulrehman T, Haik Y. Reactive extrusion of polyethylene terephthalate waste and investigation of its thermal and mechanical properties after treatment. *Int J Chem Eng.* 2017;2017:5361251.
29. Novello MV, Carreira LG, Canto LB. Post-consumer polyethylene terephthalate and polyamide 66 blends and corresponding short glass fiber reinforced composites. *Mater Res.* 2014;17(5):1285-94.
30. DEMİREL B, Yaraş A, Elçiçek H. Crystallization Behavior of PET Materials. *BAÜ Fen Bil. Enst. Dergisi Cilt.* 2011;13(1):26-35.
31. Park J-S, Park J-W, Ruckenstein E. Thermal and dynamic mechanical analysis of PVA/MC blend hydrogels. *Polymer (Guildf).* 2001;42(9):4271-80.
32. Ioakeimidis C, Fotopoulou KN, Karapanagioti HK, Geraga M, Zeri C, Papathanassiou E, et al. The degradation potential of PET bottles in the marine environment: an ATR-FTIR based approach. *Sci Rep.* 2016;6:23501.
33. Andanson J-M, Kazarian SG. In situ ATR-FTIR spectroscopy of poly(ethylene terephthalate) subjected to high-temperature methanol. *Macromol Symp.* 2008;265(1):195-204.
34. Alzuhairi M, Al-Ghaban A, Almutalabi S. Chemical recycling of polyethylene terephthalate (waste water bottles) for improving the properties of asphalt mixture. In: *The 3rd International Conference on Buildings, Construction and Environmental Engineering, BCEE3-2017 - MATEC Web of Conferences;* 2017; Sharm el-Shiekh, Egypt. *Proceedings. Sharm el-Shiekh, Egypt: EDP Sciences - France;* 2018;162: 01042.
35. Vieira SMM, Knop MC, Mesquita PL, Baston EP, Naves FL, Oliveira LFC, et al. Physicochemical properties of a solid fuel from biomass of elephant grass charcoal (*Pennisetum Purpureum* Schum.) and recyclable pet and HDPE. *Mat Res [online].* 2020;23(4):e20190350. <https://doi.org/10.1590/1980-5373-mr-2019-0350>.
36. Park E-S. Morphology, mechanical, and dielectric breakdown properties of PBT/PET/TPE, PBT/PET/PA66, PBT/PET/LMPE, and PBT/PET/TiO<sub>2</sub> blends. *Polym Compos.* 2008;29(10):1111-8.